Development of a functional stack of soil microbial fuel cells to power a water treatment reactor: from the lab to field trials in North East Brazil

Jakub Dziegielowski[1,2], Benjamin Metcalfe[2,3], Paola Villegas-Guzmán[4], Carlos A. Martínez-Huitle[5], Adryane Gorayeb[6], Jannis Wenk[1], Mirella Di Lorenzo[1,2]*

[1]*Department of Chemical Engineering, University of Bath, BA2 7AY, Bath, UK*

[2]*Centre for Biosensors, Bioelectronics and Biodevices, University of Bath, BA2 7AY, Bath, UK*

[3]*Department of Electronic and Electrical Engineering, University of Bath, BA2 7AY, Bath, UK*

[4]*Centro de Investigaciones UNINAVARRA – CINA, Fundación Universitaria Navarra – UNINAVARRA, Calle 10 No. 6 - 41. Primer piso, Neiva – Huila, Colombia*

[5]*Instituto de Química, Universidade Federal do Rio Grande do Norte, Lagoa Nova CEP 59078-970, Natal, Brazil*

[6]*Departamento de Geografia, Universidade Federal do Ceará, Campus do Pici, Fortaleza, Brazil*

* Corresponding Author: m.di.lorenzo@bath.ac.uk

GRAPHICAL ABSTRACT

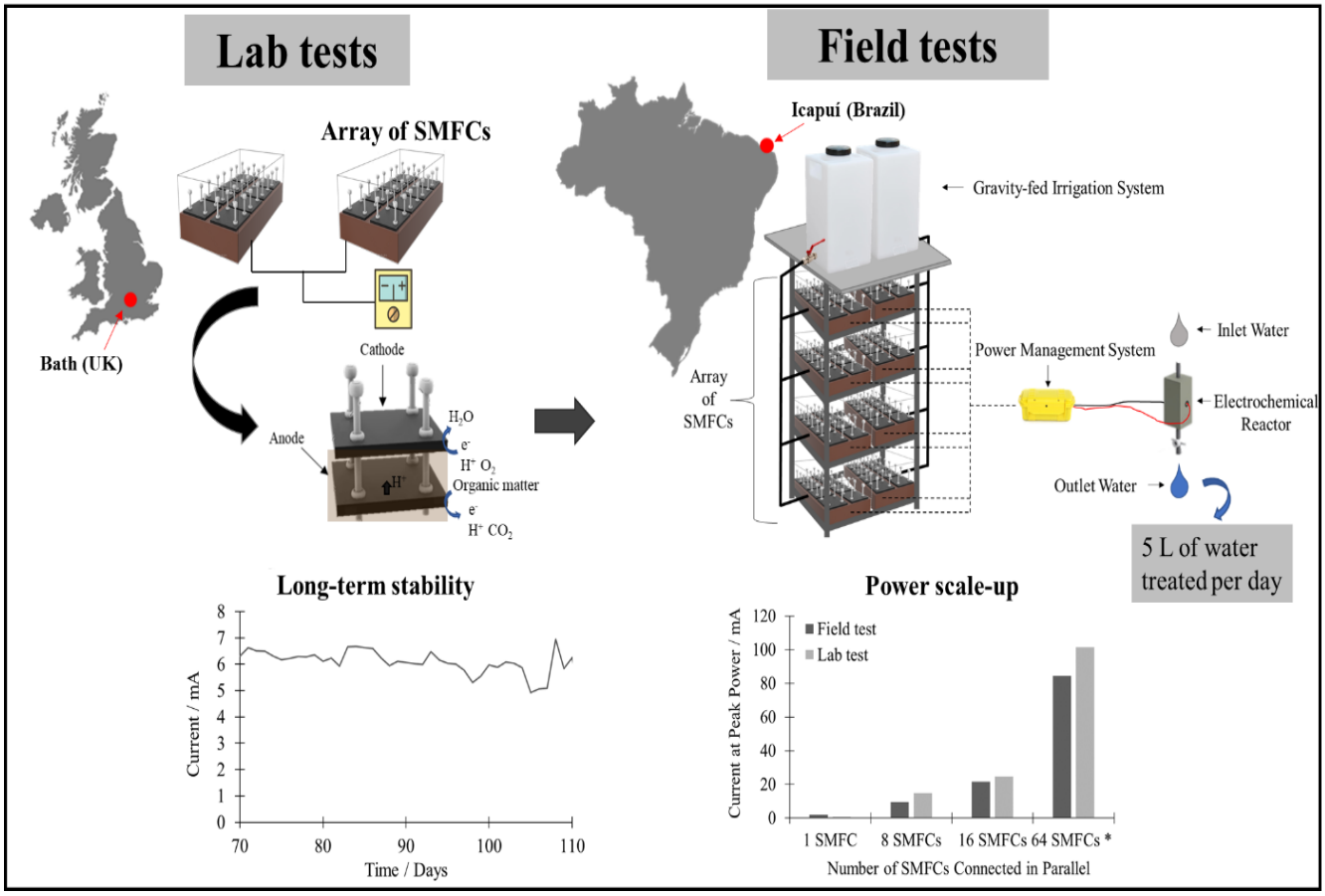

Abstract

Worldwide over 700 million people lack access to energy and safe water, while population growth and climate change further stress limited freshwater reserves. The search for innovative, sustainable, and cost-effective self-powered and decentralised water treatment technologies is, therefore, more urgent than ever; especially in vulnerable areas like North East Brazil, where water access is heavily restricted. In this context, in this study the development and implementation from the lab to the field of a low-cost, self-powered system for the decentralised treatment of water, is presented for the first time. The system consists of an array of soil microbial fuel cells (SMFCs) that powers an electrochemical reactor for water treatment. Each SMFC is characterised by a flat geometry, with the anode embedded into the soil and the cathode exposed to air. The soil acts as the electrode separator and as a source of both electroactive bacteria and organic matter. Each SMFC generates a power of 0.4 mW, which is increased up to 12.2 mW by electrically connecting 16 SMFCs in parallel, with stable performance over 140 days of operation. An upscaled system consisting of a stack of 64 SMFCs was subsequently installed at a primary school in Icapuí, North-East of Brazil, demonstrating a treatment capacity of up to three litres of water per day when integrated with the electrochemical reactor. By demonstrating implementation from the lab to the field, our work provides an effective route for the scalability and practical application of SMFC stacks for energy generation and self-powered water purification in remote areas.

Keywords: Renewable Energy; Electrochemical Water Treatment; Soil Microbial Fuel Cells; Scale-up; Power Management System, Sustainability

Introduction

Access to both sustainable energy and safe water are two global targets set by the United Nations Sustainable Development Goals (SDG) for 2030, which are tightly connected to each other. Despite being both a fundamental human right, over 700 million people (11% of world's population) still suffer from energy and water scarcity (1). Factors such as population growth, rapid urbanisation, climate change and environmental pollution put freshwater resources under threat while pushing for more reliable and affordable energy solutions. Some of the most vulnerable communities around the world are also those that suffer the most direct consequences from the shortage of energy and safe water. For example, energy and water scarcity in the North East regions of Brazil creates extreme social and economic vulnerability. These areas suffer from a semiarid climate and water resources that are frequently polluted by unsustainable human activities (2). In North East Brazil, and other areas worldwide that share similar challenges, the development and implementation of self-powered, sustainable, affordable and innovative technologies for decentralised water treatment is, therefore, critical.

Electrochemical treatment (ET) technologies have shown great potential for water purification and disinfection (3-5). Key advantages over traditional methods are high efficiency, mild operating conditions, and great versatility (6). A disadvantage of ETs is their relatively high-power requirements, which makes this technology impractical in areas where a stable energy supply cannot always be guaranteed. Thus the integration of ETs with renewable energy sources is key for scalability and implementation in remote areas (7). Microbial Fuel Cell (MFC) technology holds great potential as a low-cost and sustainable power source that might be used to power ETs, as recently shown by coupling an electrochemical reactor with an array of MFCs for algae removal in wastewater (8). MFCs are fuel cells in which microorganisms catalyse the direct conversion of organic matter into electricity. A range of wastewaters have been used as effective fuel source for MFCs, thus demonstrating not only the technology potential as a carbon-neutral and green energy source, but also significant versatility (9). Wastewater treatment by MFCs has been widely demonstrated, particularly BOD and COD removal (10), water denitrification (11) and, recently, pathogens removal (12). MFC technology is, however, less effective than ET methods, such as Fenton-based advanced oxidation, which are able to treat water to a higher quality standard, by generating powerful hydroxyl radicles and are also suitable for drinking water treatment (13).

With regard to the use of MFCs as a power source, several studies have demonstrated the possibility to scale-up the output power by stacking together multiple MFC units (14).

Moreover, the use of a power management system can ensure effective and stable performance over long periods of time (15). Soil Microbial Fuel Cells (SMFCs) are a specific class of MFCs in which the soil acts as the supporting matrix, the source of microorganisms, and, in membrane-less configurations, also as the separator between the anode and the cathode (16). Consequently, the overall design of SMFCs is simpler and easier to scale up than traditional MFCs (17). Furthermore, in SMFCs there is no need for external fuel provision, as in other types of MFCs, which further simplifies the system operation, since the organic matter, generated through the action of organisms present in the soil is transported to the anode by diffusion through the soil (18). SMFCs are consequently a good candidate for cost-effective power generation in remote areas, where low maintenance is preferable.

Traditionally, benthic and sediment MFCs, with the anode embedded in sediment and the cathode suspended in water, have been widely tested in field (19). Initial prototypes implemented in marine sediments achieved power densities of up to 20 mW m^{-2} (20), which has been further increased to 100 mWm^{-2}, with design optimisation (21). Such a high performance has, however, only been reached in a laboratory setting for no more than 45 days, as these systems often struggle with high ohmic losses, caused by significant electrode spacing and fouling (21). Apart from marine sediments, similar configurations have been tested in wetlands (22) and paddy fields (23), reaching maximum power densities of 18 mWm^{-2} and 14 mWm^{-2}, respectively. Usually, these devices are based on a flat geometry and some integrate compost (24) or plants (25) to provide additional organic matter and enhance the performance. Although effective, with some cases reporting 240% increase in power densities, from 5.13 to 12.42 mWm^{-2} (26), utilization of plants has shown to have negative impacts on stability, due to the influence of sunlight on the electric output (27). To minimise ohmic losses, and eliminate the sunlight-dependent electricity generation, a tubular design installed in a wetland has also been recently proposed (28). In this design, the anode was wrapped outside the tubular support and the cathode was placed inside, exposed to air. Despite achieving a smaller footprint and greater power performance of 22 mWm^{-2}, this device suffered from instability due to oxygen crossover from cathode to anode, significantly lowering the electric output over the period of 160 days (28). Operation in waterlogged environments helps maintain the anode under anoxic conditions whilst facilitating ion transport to the cathode (29). It often implies, however, that the cathode is fully submerged in the water, which slows down the oxygen reduction kinetics and leads to the need for expensive catalysts or additional aeration (30). In SMFCs designs with the cathode exposed to air, performance can be greatly affected by the moist content in

soil. Scale-up and field implementation of the technology must necessarily account for operations in a moist-controlled environment.

In this work, we present the development and transition from the lab to the field of a cost-effective array of SMFCs to generate energy and power an electrochemical reactor for water treatment. Each SMFC has a flat geometry, with the anode embedded into the soil and the cathode exposed to air. The moisture content within the soil can significantly affect the performance of SMFCs with air exposed cathodes, and so to control the moisture content the soil in which the SMFCs were operated was placed in a box and a gravity fed irrigation system was implemented. The power output is scaled up by electrically connecting multiple SMFCs in parallel; the effect of operating the SMFCs in a shared or independent electrolyte configuration was also investigated. To harvest the energy generated by the stack and store it until required, a power management system is used and its operation characterised. Finally, the SMFC stack was integrated with an electrochemical reactor to demonstrate the self-powered treatment of pond water in a primary school in North East Brazil. Consequently, this study shows for the first time the effective upscaling of SMFCs for energy harvesting and the self-powered electrochemical treatment of water in remote areas.

Materials and methods

Materials

All reagents used were purchased from Alfa Aesar and Sigma-Aldrich of analytical grade and used without further purification.

The lab-based tests were performed with soil collected from the University of Bath campus. Prior to use, the soil was cleaned from small stones, roots, and leaves. No external organic matter was added. The nitrogen (N), phosphorous (P) and potassium (K) content in the soil was qualitatively assessed with the HI-3869 Soil Test Kit (Hanna Instruments), using the provided guide (31). The pH and conductivity of the soil were measured by using a Thermo Scientific Orion Star A325 probe. The initial water content of the soil, WC_{soil}, was determined from the weight difference before and after a drying process, according to Equation 1:

$$WC_{soil}(\%) = \left(\frac{W_1 - W_2}{W_2}\right) * 100\% \qquad (1)$$

where, W_1 and W_2 is the weight (g) of the soil sample respectively before and after being oven-dried overnight at 105°C (32).

The percentage of organic matter content (OM) of the dried soil samples was analysed by the Loss of Ignition (LOI) method (33). Briefly, the samples where were heated to 375 ºC for 24 h and the OM was calculated according to Equation 2:

$$OM = \left(\frac{W_b - W_a}{W_b}\right) * 100 \quad (2)$$

where W_b and W_a is the weight (g) of the soil sample respectively before and after ignition.

In the field tests commercial agricultural soil was purchased from a local gardening centre in Fortaleza, Brazil (MF Rural). Table 1 summaries the physicochemical characteristics of both soils used in the study, obtained through lab analysis and specified by the manufacturer.

Table 1. *Physicochemical properties of the soil used in the laboratory and field tests*

Parameter	**Laboratory tests**	**Field tests**
pH	6.5	7
Nitrogen	Low: < 10 ppm	Medium: 10 – 20 ppm
Phosphorous	Trace: < 10 ppm	Medium: 20 – 40 ppm
Potassium	Low: < 150 ppm	Medium: 150 – 250 ppm
Moisture content	53 %	55 %
Organic matter content	17.4 ± 1.5 %	25.8 %

Soil Microbial Fuel Cell Design and Operation in Laboratory Experiments

The SMFCs developed in this study consisted of two graphite felt electrodes (10 x 10 x 0.7 cm) separated by a fixed distance of 4 cm with 10 cm long nylon screws (Bluemay Ltd), as shown in Figure 1A. To understand the most effective design for technology scale up, SMFCs with lager electrodes were also tested, with dimensions of 27.5 x19.5 x 0.7 cm ($SMFC_{Large}$), shown in Figure 1B. In all cases, no external membrane was used and at the cathode, no oxygen reduction reaction catalyst was implemented. Before use, the anodes underwent an acid and heat treatment to increase the hydrophilicity and the roughness of the carbon nanofibers, as previously described (34).

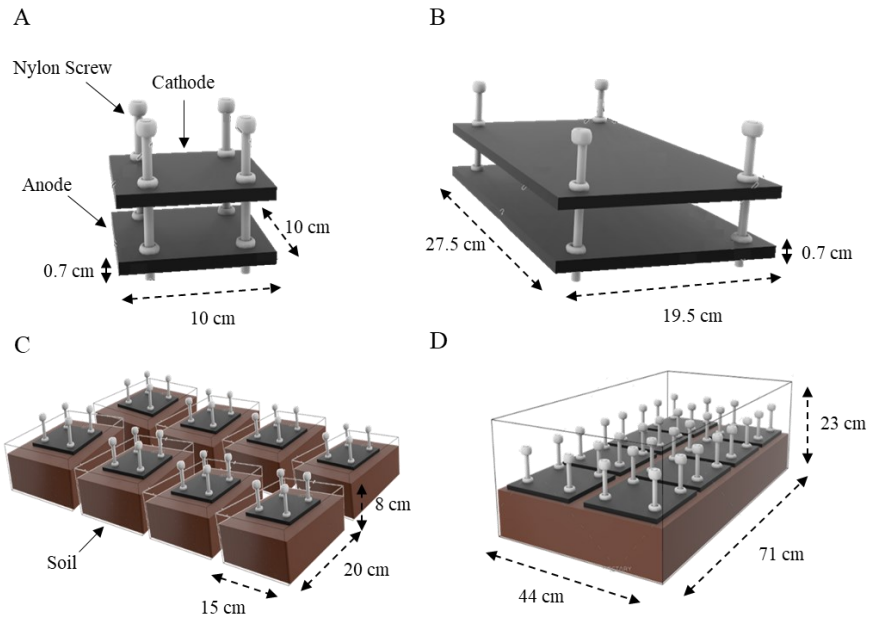

Figure 1. Sketch of the two SMFC designs used and experimental set-up. A) SMFC with small electrodes; B) SMFC with large electrodes; C) operation in individual boxes; D) operation in shared electrolyte.

The performance of the SMFCs was investigated both in individual and shared electrolyte conditions. With this purpose, 16 soil microbial fuel cells with small electrodes were constructed (Figure 1A). Eight SMFCs were placed in separate 20 x 15 x 8 cm PVC containers and the other eight were kept in a single 71 x 44 x 23 cm box, as shown in Figure 1C and 1D respectively. The devices with large electrodes, $SMFC_{Large}$, were also fit into individual boxes of dimensions 35 x 25 x 8 cm. In each case, the cathode was exposed to air and the anode buried into the soil. The electrodes were manually woven with titanium wire (0.25 mm diameter), which acted as the current collector. Each SMFC was connected to an external resistance of 510 Ω, and to a data acquisition system (ADC-24 Pico data logger, Pico Technology, UK).

The PVC containers were installed into a two-level frame with LED lights; the lighting was ON/OFF for 12/12-hour cycles to simulate day and night conditions, at room temperature (20 ± 2 ºC). To maintain the moisture content the soil was irrigated with approximately 1.5 L of tap water every 48 h using a gravity fed irrigation system, comprising of a 25 L water tank (TanksDirect), an electronic water timer (Kingfisher) and a micro drip irrigation kit (Yikaich), see Figure S1B in the Supplementary Data for more detail.

Analysis

During the enrichment stage, the output voltage, E, generated by the fuel cell over time was interpolated with the modified Gompertz model, according to Equation 3 [31].

$$E = E_{max} \cdot \exp\left(-\exp\left(\frac{\mu_{max} \cdot e}{E_{max}}\right) \cdot (\lambda - t) + 1\right) \qquad (3)$$

Where: E_{max} is the steady-state cell voltage (V); λ is the lag phase duration (days); e is the Napier's constant (2.71828); μ_{max} is the maximum specific growth rate (d^{-1}).

Once a steady state voltage output was observed (approximately after three weeks), the SMFCs were electrically stacked in parallel to scale-up the power output.

Polarization tests were performed by connecting the SMFCs to a decade resistance box (Cropico RM6 Decade), varying the applied resistance, R, from 900 KΩ to 40 Ω every 10 minutes, and recording the pseudo-steady state output voltage. Ohm's law, $E=IR$, was used to calculate the corresponding current (I) at each external load value. The power, P, was calculated using the power law, $P=IE$.

Operation of the electrochemical reactor for water treatment

Water purification by advanced oxidation was performed with a commercial electrolysis reactor, Mini-DiaCell® (Adamant Technologies). The electrochemical cell consisted of two Boron Doped Diamond (BDD) electrodes of dimensions 2.5 x 5.5 cm, secured inside a 9 x 4 x 4.5 cm case, with pre-drilled holes for water inlet and outlet, as well as for the electrical connections.

To avoid power requirement associated with pumping, a gravity driven set-up was developed, as shown in Figure S2. This consisted of a 1 L funnel attached at the top of the reactor, where water was stored prior to treatment, and a valve at the outlet, installed with the purpose of controlling the flow rate/hydraulic retention time.

The optimal operating conditions for the reactor, in terms of both current applied and hydraulic retention time, for effective water treatment were investigated with a synthetically contaminated water. The aqueous solution contained 10 ppm of methyl orange and 0.05 M of Na_2SO_4 and was made with distilled water. Sodium sulphate was used to enhance the conductivity of the solution, facilitating the electrochemical reactions, whilst methyl orange was used as a model pollutant, due to the ease of monitoring its degradation using UV spectroscopy (35). Thus, removal efficacy was assessed in terms of absorbance (Abs) variation between inlet and outlet at the wavelength of 464 nm, according to Equation 4:

$$removal\ efficiency = \frac{Abs_{in} - Abs_{out}}{Abs_{in}} * 100 \quad (4)$$

The absorbance was measured with a UV-Vis Spectrophotometer (Agilent Technologies). Current was supplied using a power source (Topward Electric Instruments co. ltd.), whilst the flow rate was adjusted manually with a valve. The two parameters were then used to estimate the volume of water treated, as per Equation 5:

$$V_{H_2O} = \left(\frac{C}{P_r - P_{SMFC}}\right) * Q \quad (5)$$

Where V_{H2O} is the volume of treated water (L), C is the total energy delivered (mW h), P_r is the power required by the reactor (mW), P_{SMFC} is the power continuously generated by the fuel cells (mW) and Q is the flow rate (L h^{-1}).

Power management system

To harvest, store and supply energy from the SMFCs and meet the energy requirement of the electrochemical reactor, a power management system (PMS) was developed. The complete electronic circuit consisted of four stages: a BQ22504 boost converter and battery charger; a 3.6 V battery; a MAX17250 boost converter, and an LT3092 constant current source (Figure 2).

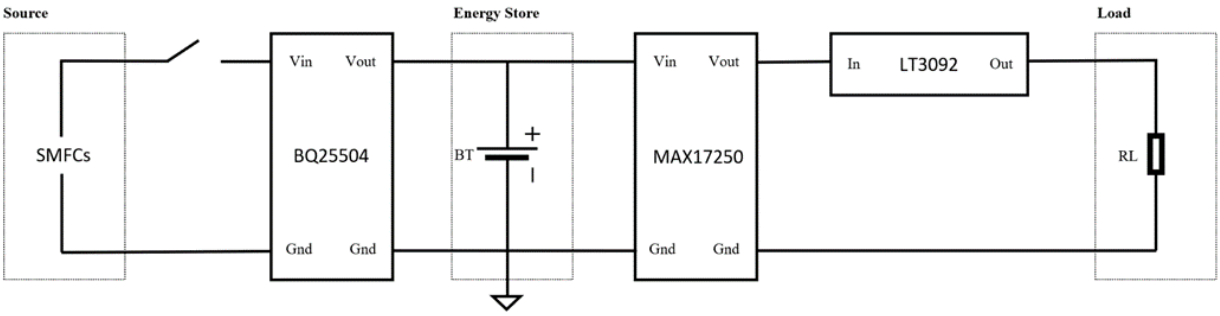

Figure 2. Electronic circuit of the power management system used in this study.

In the first stage, the SMFCs were connected directly to a BQ25504 boost converter (Texas Instrument), an energy harvester specifically designed to efficiently acquire and manage micro to milliwatts of power from variety of DC sources (36). The harvested energy was then used to charge a 3.6 V, 600 mAh (NiMH) nickel metal hydride battery stack, comprising of three single cell batteries connected in series with a nominal voltage of 1.2 V each. This battery was chosen as the energy storage element since its capacity provides sufficient energy to purify over 1 L

of water. The battery has a maximum charged voltage within range of the output of the BQ25504 and can be protected from under or over charging. Since the source voltage coming from the battery was too low to meet the reactor operating conditions, in the third stage of operation, a boost converter (MAX17250 – Maxim Integrated) was added to step-up the voltage and generate an output of 18 V. Lastly, before connecting the PMS to the electrochemical reactor, the current supply was fixed with a constant current source (LT3092 – Linear Technology). This step ensured that a constant current of 200 mA was delivered to the reactor despite changes in load impedance, thus maintaining uniform performance of the water treatment process. To guarantee safe and reliable field operation, all the electronic components were placed in an IP67 box, designed to prevent ingress of water, dust and any other potential contaminant.

The performance of the PMS was assessed in terms of battery charge and discharge tests. Prior to the charge tests, the battery was drained below its nominal point, to be able to distinguish the percentage charge remaining inside more accurately. This was done by connecting the PMS to a load, such as a small fan, and running it until the desired battery voltage is reached. After that, the SMFCs were connected to the PMS and left to charge the battery, whilst the battery voltage was monitored with a multimeter (Sealey). The discharge tests were performed once a full charge was reached. Then, the PMS was connected to a load and the output current and voltage were measured. All results were then normalised to a single cell battery (1.2 V) and compared against a discharge curve provided by the manufacturer (Figure S3).

Field work: experimental Set-up and Operation

The field work was performed in the courtyard of the primary school EEF Professora Mizinha of Icapuí, State of Ceará, Brazil (4°42'23.94"S 37°21'39.43"W). Eight SMFCs (electrodes size 10 x 10 x 0.7 cm) were fit into 50 L (23 x 44 x 71 cm) PVC boxes filled with soil, for a total of 8 boxes and 64 SMFCs. The boxes were distributed onto the shelves of two frames, which were placed in the school courtyard (see Figure S1D). During the operation, the soil moisture content was maintained with pond water collected nearby the school (pH 7.5 ± 0.3, salinity 0.3%, dissolved oxygen 3.3 ± 0.1 mg L^{-1}). A gravity fed irrigation system was set-up on the top shelf of the two frames. The average temperature during the experiments was 30 ℃, with an average humidity of 80 %.

As for the case of the lab experiments, the SMFCs were enriched with an individual electrical connection for 14 days using an external resistor of 510 Ω. Subsequently, the SMFCs were

electrically connected in parallel. The output voltage was monitored discretely by means of a multimeter (Sealey). Polarization tests were performed by connecting the fuel cells to a data logger and monitoring pseudo steady state voltages under different external resistances.

For the water treatment tests, the stack of 64 SMFCs in parallel was connected to the PMS to charge the battery. Afterwards, the stored energy was used to power the electrochemical reactor and drive the electrochemical purification of water. To assess the efficacy of treatment, dissolved oxygen content was measured in both the inlet and outlet water with a multiparameter by Hanna Instruments.

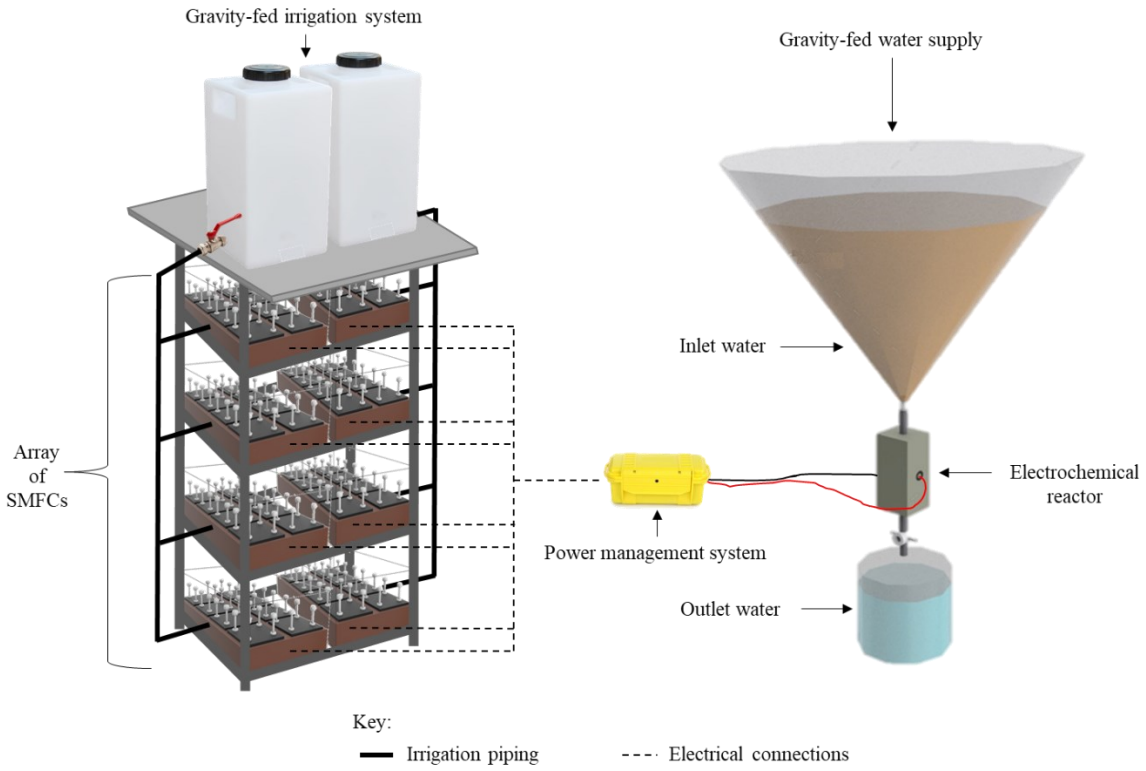

Figure 3. Experimental set-up of the self-powered water purification system (not to scale).

Results and Discussion

SMFC configuration and power scale-up

The aim of this study was to demonstrate the self-powered electrochemical treatment of water by coupling an electrochemical reactor with a stack of soil microbial fuel cells. The integrated system was firstly developed and tested in the lab and then tested in field.

Initial tests investigated the most effective set-up for energy generation by the SMFCs. In the design presented the soil acts as the supporting matrix, the electrode separator, and as the source of electroactive bacteria and organic matter. Previous studies have reported a potential drop in fuel cell stacks with a shared anolyte configuration, due to ionic cross conduction and the parasitic current generated (37, 38). Therefore, tests using both individual or shared anolyte were carried out, as detailed in the Methods Section, to understand the effects that each arrangement would have on the generated power.

Figure 4 shows the enrichment curves and the power curves of the SMFCs in both a shared and non-shared anolyte configuration. No marked difference in the start-up time, power generation and internal resistance (Figure S4), was observed between the two configurations. On average each fuel cell generated power densities of 38 mWm^{-2}. Still, the individual anolyte configuration showed greater variation between each box, probably because of difficulties in maintaining uniform soil moisture in the individual boxes.

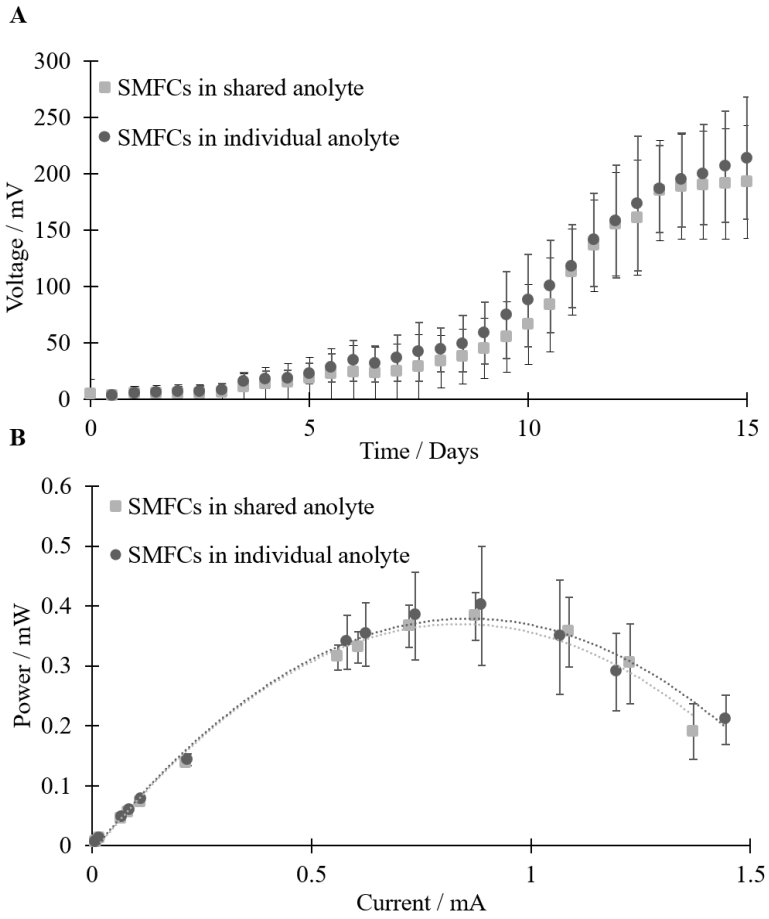

Figure 4. Electrochemical performance of the SMFCs operated in a single large box (shared anolyte configuration) and in individual boxes (individual anolyte configuration). A)

enrichment curves over 15 days. B) power curves obtained from polarisation tests. Error bars refer to 8 and 4 replicates respectively for the case of shared and non-shared electrolyte.

After 38 days of operation, the SMFCs in both configurations were electrically connected in parallel. First, a stack of two fuel cells only was established. After every 48 h, an additional fuel cell was connected and so on until a stack of eight fuel cells was obtained. As expected, this strategy led to an increase of the power density from 38 mWm^{-2} to 75 mWm^{-2}, which enabled a linear scale-up in the power output (Figure 5). In the case of the SMFCs in the shared anolyte configuration, the power output increased more than eight times with a stack of eight SMFCs, i.e. from 0.38 mW to 6.54 mW. For the case of the SMFCs in the individual electrolyte configuration, the peak power obtained with the stack of eight SMFCs was 1.13 times smaller, which was due to the non-uniform performance of individual units.

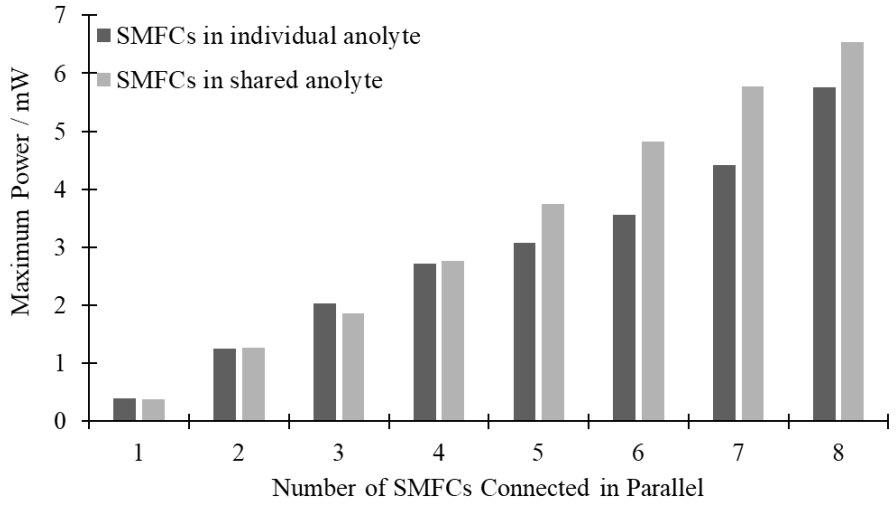

Figure 5. Peak power output of stacked SMFCs in both individual and shared anolyte conditions obtained through polarisation tests. The polarisation was performed two days after electrically connecting in parallel the SMFC units, and each time the applied external resistance was adjusted to the optimal value.

Sharing the electrolyte did not affect the performance of the SMFCs. In fact, when the SMFCs were connected in stack, the shared electrolyte configuration led to greater power outputs.

To further examine possibilities of optimising the design and to understand the best route for power scale-up, the use of a large fuel cell was also tested. The resulting performance was compared with an array of SMFCs connected in parallel with an equivalent geometric surface area of the electrodes. It has been previously demonstrated that in continuous flow systems, the miniaturisation and multiplication strategy is an effective route for scaling-up (39). In continuous flow systems, a design characterised by short electrodes would reduce the thickness of the diffusion layer developing along the electrode length, leading to better fuel efficiencies (40). This approach may, however, not be valid in our system, as the fuel provision relies on diffusion through the soil rather than external feeding.

To verify this hypothesis, two SMFCs with larger electrodes, $SMFC_{Large}$, were built and tested as alternative to the stack of multiple SMFCs units with smaller electrodes. Both the anode and the cathode in $SMFC_{Large}$ were equivalent to five electrodes (in terms of geometrical size) used in the other SMFCs. Figure 6A shows a comparison of enrichment curves for SMFCs with small and large electrodes. For $SMFC_{Large}$ the lag phase is shorter, approximately 3 days, and the steady-state voltage is reached after only 8 days rather than 13 days. Such substantial reduction in start-up time is a result of a lower internal resistance, due to the electrodes size (41). Nonetheless, the steady state voltage generated by $SMFC_{Large}$ (284 ± 16 mV) was approximately 1.4 times larger than the one generated by SMFCs with smaller electrodes (207 ± 62 mV), and the power density dropped to 5.8 mWm^{-2}, showing a negative trend versus electrode surface area. Moreover, when five SMFCs were connected in parallel, leading to electrodes with the same equivalent geometric area of $SMFC_{Large}$, the resulting peak output power (3.66 mW) was approximately 12 times larger than $SMFC_{Large}$ (0.31 mW), as shown in Figure 6B.

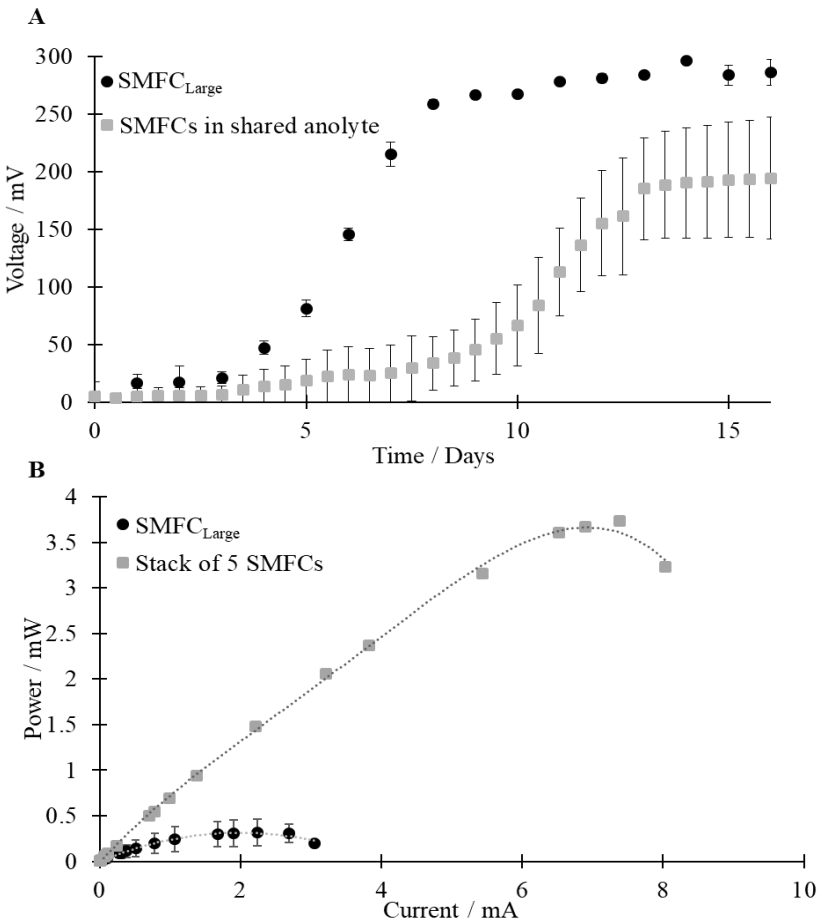

Figure 6. Effect of increasing the electrodes size, comparison of performance. A) Enrichment curves of $SMFC_{Large}$ (n=2) and SMFC (n=8) operated under the external load of 510 Ω. In $SMFC_{Large}$, both the anode and the cathode are five times larger than in SMFC. B) Power curves obtained from polarisation tests. Comparison between $SMFC_{Large}$ (n=2) and a stack of five SMFCs connected in parallel (n=1), leading to a surface area of the electrodes equivalent to those in $SMFC_{Large}$.

The poor performance of $SMFC_{Large}$ may be attributed to current losses within the electrode (42). In the case of the cathode, it was also challenging to ensure contact of the electrode and the soil. Similar findings by others suggest that the relationship between power density and surface area of the current-limiting electrode is non-linear, due to edge effect and mass transport limitation (43). Nonetheless, the polarisation tests showed that both $SMFC_{Large}$ and the stack of five SMFCs were characterised by an internal resistance of approximately 60 Ω, (see Figure S5), which seems to contradict the design fault hypothesis. A more systematic

investigation, beyond the scope of this study, should be performed to further explore this phenomenon.

Considering these results, all other experiments were performed with stacks of small sized SMFCs in shared electrolyte. To assess the long-term performance, SMFCs previously operated in individual boxes were moved into a single large container, leading to a second stack of eight SMFCs. Three weeks later, the two stacks of eight SMFCs in shared electrolyte configuration were connected in parallel. The resulting stack system generated a peak power of 12.2 mW or 76.3 mWm^{-2} (Figure S6), further confirming the linearity of the strategy adopted for the power scale-up. The stack was also capable of sustaining continuous powering of a white LED, as shown in Figure S7.

The SMFCs were then left to operate under a 100 Ω load, instead of the resistance value at which maximum power was obtained (20 Ω). This strategy was adopted to avoid excessive stress to the anodic microbes (44). Figure 7 shows that the performance of the stack was very stable over time, generating a current density of approximately 40 mAm^{-2} (6.1 ± 0.3 mA), which is in line with what has previously been reported in plant MFCs (45). The current drop observed on day 110 of operation was caused by a fault in the irrigation system, resulting in no watering of the boxes for up to five days. Once the issue with the irrigation system was solved, the baseline current was re-established. Due to time restrictions, the experiment was stopped after 140 days of operation. Nonetheless, the performance of the SMFCs stack was sustained during this period of time. Compared to plant MFCs that have shown long-term performance deviations of over 90 %, related to sunlight dependence (27), or in the case of tubular designs, to oxygen crossover (28), our SMFCs demonstrated a much more resilient operation. Furthermore, unlike conventional or floating MFCs (46), exposed to a greater variation in organic content, pH and flow rate of the wastewater (10), the semi-controlled environment in our system helped generate steady power, representing a viable option for a stable long-term operation.

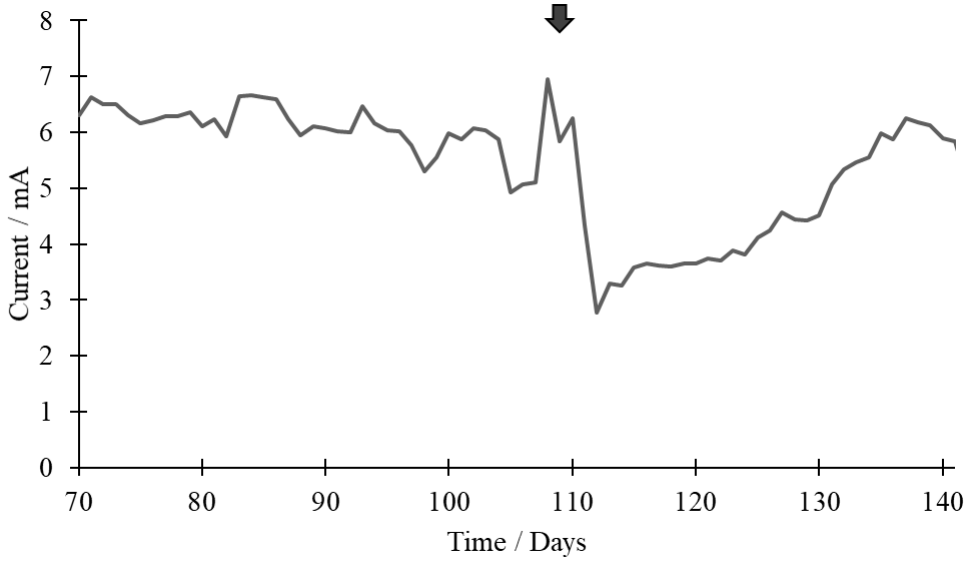

Figure 7. Current generated over time by the stack of 16 SMFCs electrically connected in parallel under a 100 Ω load. The arrow indicates the point where the irrigation was interrupted. After five days, the system was watered again.

Operational conditions of the electrochemical reactor

Prior to field testing, the operational conditions of the electrochemical reactor were optimised in the lab. The applied current was investigated to confirm the electrochemical production of oxidizing species that would enhance the treatment efficacy (47). Another important factor is the retention time within the reactor, with longer times being more beneficial to the treatment, because the oxidizing species react with the pollutants in the reaction cage, favouring a complete elimination (47). To address the overall energy demand of the reactor with the SMFCs stack and develop a self-powered integrated system, the most energy efficient combination between these two factors had to be investigated. With this purpose, three different flowrates (7 ml min^{-1}, 13 ml min^{-1} and 17 ml min^{-1}) were tested at different power ratings. At an operating voltage of 8 V, an applied current of either 100 mA, 200 mA or 240 mA was selected to achieve a treatment efficiency (i.e. percentage of methyl orange dye removed, Equation 4) no lower than 90%.

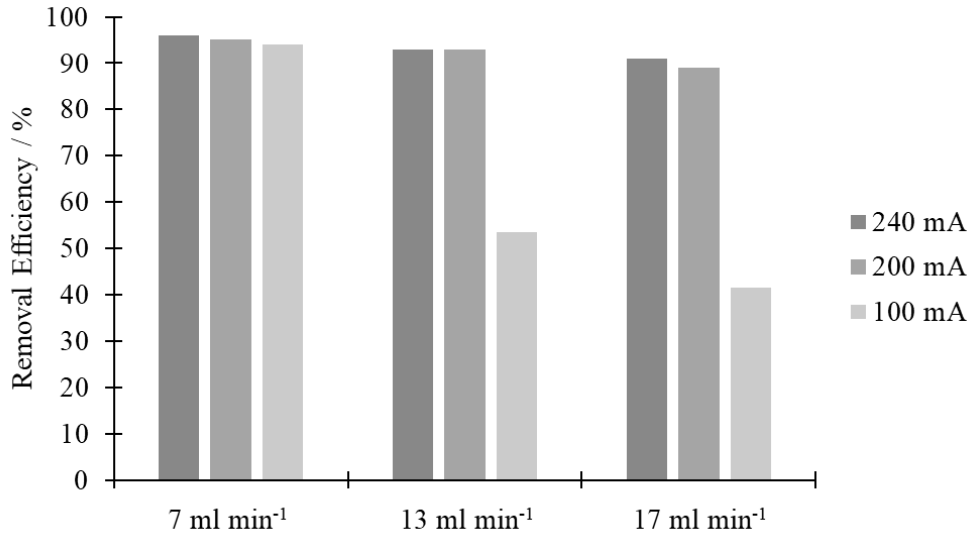

Figure 8. Optimising the operational parameters of the electrochemical reactor.

As expected, the highest removal efficiency obtained, 96%, occurred at the highest input current (240 mA) and the slowest flowrate (7 ml min^{-1}) tested (47). This result clearly indicates that sufficient oxidizing species (hydroxyl radicals) are produced at the BDD surface by applying higher current, to promote the electrochemical incineration of the organic pollutant due to the higher residence time with the oxidants in solution. Under this flowrate and applied current, the treatment of 0.5 L of water would take approximately 1.2 h. To sustain the reactor operation for such duration, a 600 mAh 3.6 V NiMh battery would be required as the energy storage component. Nonetheless, by supplying a current as low as 100 mA to the reactor, under the same flowrate, the removal efficiency was maintained at 94%. With the lowered current demand, a battery of the same capacity could sustain the reactor for up to 2.9 h, allowing for treatment of 1.2 L of water.

Although slower flowrates would enhance the treatment efficiency, thanks to a better contact between oxidants and contaminants, higher flowrates would allow the treatment of higher water loadings per unit time. For this reason, faster flowrates were also tested. As shown in Figure 8, removal efficiencies above 90% were still maintained with high current inputs. This result is due to the efficient electrogeneration of oxidizing species by using BDD anodes, as previously reported (48, 49). Considering the results obtained, a selection of 200 mA for the input energy and 17 ml min^{-1} for the flow rate (to be met by gravity flow) was selected.

SMFCs operation in field

Based on the lab results, field tests were subsequently performed in Icapuí, North-East Brazil. The aims of these tests were to investigate the stack performance with a different soil formulation, under the environmental conditions typical of semi-arid regions, and to demonstrate effective self-powered water purification by integrating the SMFCs stack with the electrochemical reactor.

As shown in Figure 9, despite differences in soil composition, water used for irrigation, operating temperature and humidity, the performance in the field was comparable to lab results, thus demonstrating good reproducibility. Under field condition it was observed that the internal resistance of a single fuel cell was 144 Ω (Figure S8), 3.5 times lower than the value obtained in the lab, and the current generated in the field was twice as high. This significant reduction of the internal resistance could be attributed to the difference in conductivity of the irrigation water used in the field. The latter, collected from a pond nearby the school, was characterised by an electrical conductivity of 4.68 mS cm^{-1}, whereas the tap water used in the lab had a conductivity of 0.32 mS cm^{-1}. Moreover, as shown in Figure 9A, in the field the steady-state voltage was reached on day 10, four days faster compared to the lab.

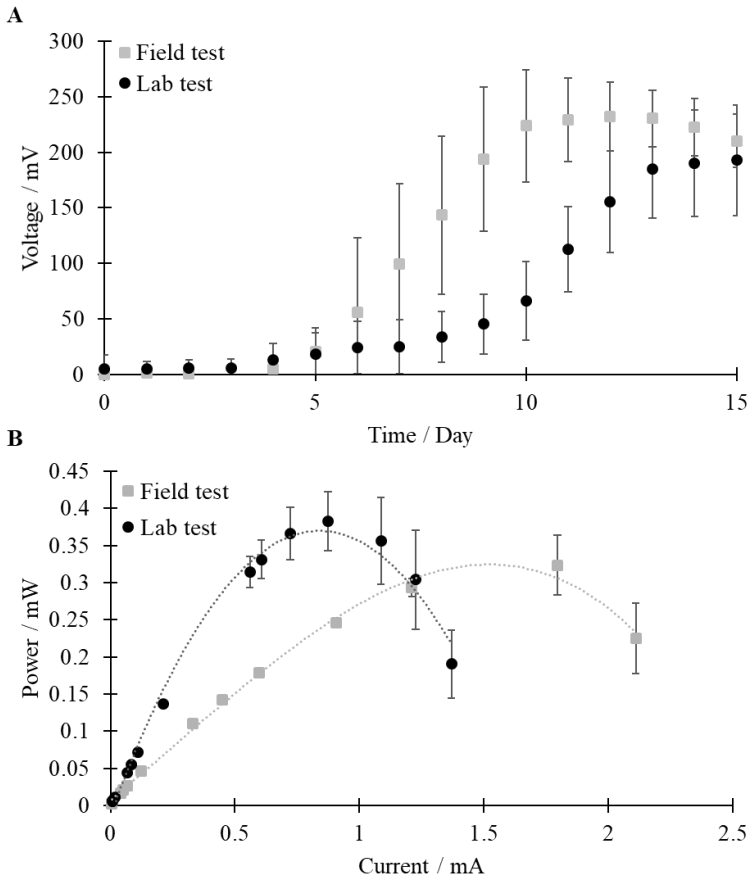

Figure 9. Comparison of performance in the lab and in the field of individual SMFCs in shared electrolyte. Data is the average of 8 replicates.

After being enriched individually, the SMFCs were connected in parallel to generate stacks of 8 first, then 16 and ultimately 64 SMFCs. Figure 10 compares the stack performance in the field with the lab.

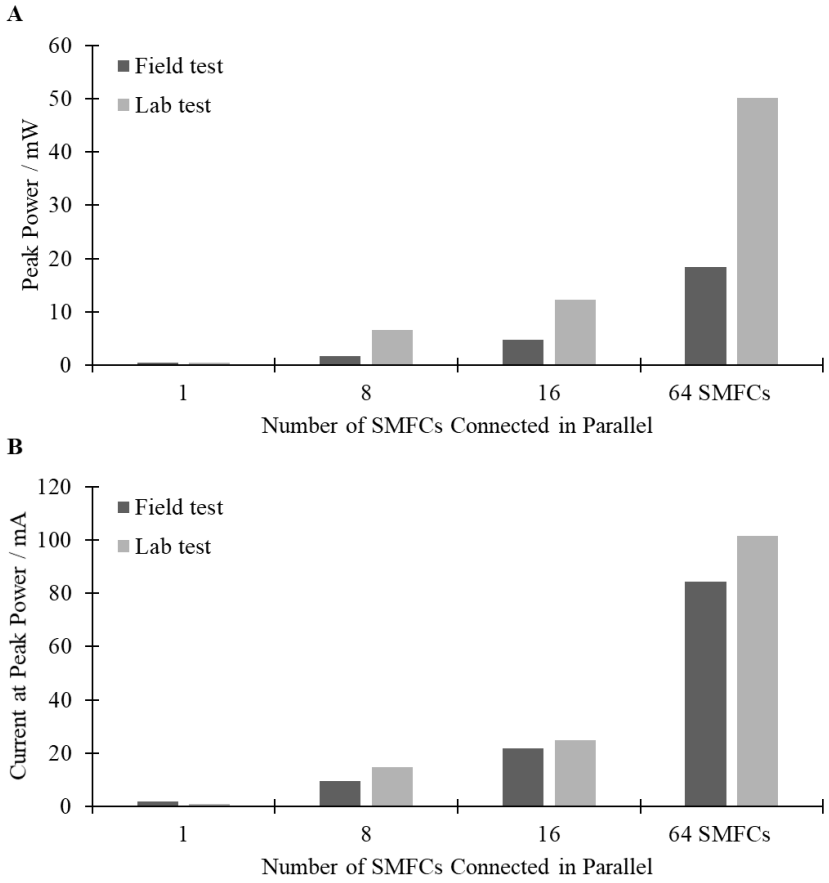

Figure 10. Comparison of performance in terms of maximum power (A) and current at maximum power point (B) for SMFCs operated in the lab and in the field. Note that results for 64 SMFCs are theoretical values extrapolated from experimental trends, as described in Fig S9.

The experiments revealed that the maximum power generated by the stack in the lab was significantly larger compared to the field-based systems. This difference was attributed to a greater cell potential. For example, the open circuit voltage for a stack of 8 SMFCs in the field was 454 mV, compared to 734 mV obtained in the lab-based set-up. One of the possible reasons

for this could be the shorter operation period in the case of the field experiments, 25 days versus 50 days in the lab-based experiments. Consequently, the anodic biofilm may have not been mature enough when these electrochemical tests were performed (50). Nonetheless, the internal resistance of the SMFCs in the field was lower, leading to the generation of a comparable current at peak power, as shown in Figure 10B.

Due to equipment restriction in the field, it was not possible to perform polarization tests on the stack of 64 SMFCs. Nonetheless, considering the linear relationship observed between current and number of SMFCs arranged in parallel (R^2 of 0.9916), extrapolation of the result suggests that the stack of 64 SMFCs would generate a peak current of 85 mA and a peak power of 18.3 mW. To test the accuracy of this estimation, the stack of 64 SMFCs was connected to the PMS and the battery charge time was measured by monitoring the battery voltage over a period of three days (Figure 11A).

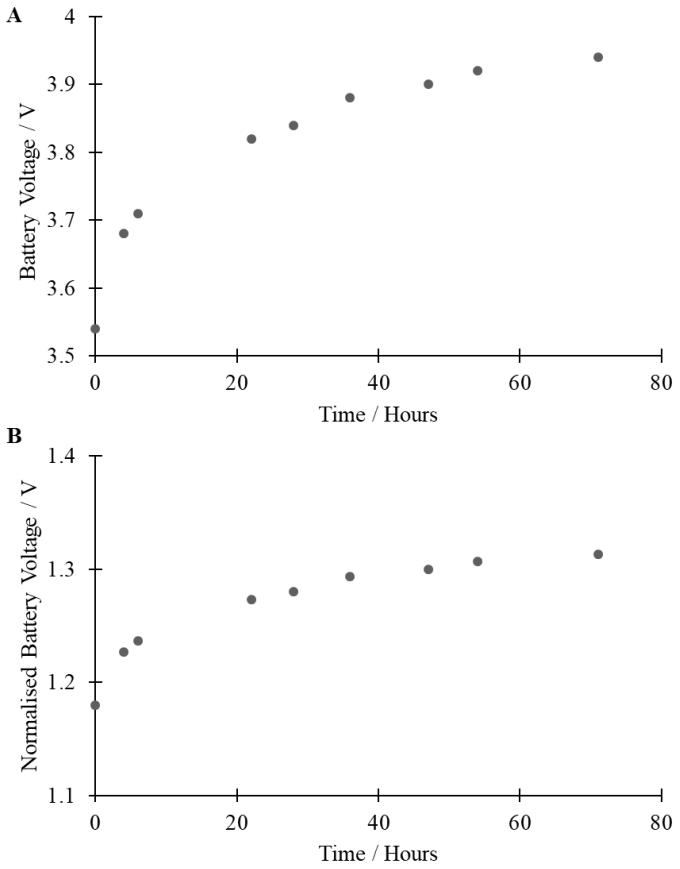

Figure 11. A) Charging behaviour of the 3-cell NiMH battery stack. B) Charging behaviour normalised to a single battery cell.

The charge test was initiated once the single battery cell equivalent voltage dropped below the nominal value, reaching 1.18 V. This voltage, compared with the discharge curve in Figure S3, at 1 CA (nominal discharge current of 100 mA), equates to 60% discharge, or 40% of full charge. At this point, the stack of SMFCs was connected to the PMS. The next measurement was taken after 4 h, showing 1.22 V, or 80% of charge. The 40% increase follows the theoretical charge rate, as the maximum time to achieve a full charge (assuming 20% efficiency loss) of a 600 mAh battery, with a charge rate current of 85 mA, was estimated to be 8.5 h, using Equation 6.

$$T_c = \left(\frac{C}{I_c}\right) \div \eta \qquad (6)$$

Where T_c is the time taken to reach a full battery charge (hr), C is the battery capacity (mAh), I_c is the current applied (mA) and Ƞ is the battery charge efficiency

The battery charging was limited to a maximum single cell equivalent voltage of 1.33 V by the PMS, and after 22 h of charging, the battery single cell equivalent voltage was 1.27 V (91% of charge). One day later, the percentage charge increased by only 2%, and finally at the end of day 3 the experiment was stopped, with the battery reaching its single cell equivalent voltage of 1.31 V or 93.5% charge. The reason for the difference between the final single cell equivalent voltage and the pre-set limit is likely down to tolerances in the resistor values used for setting the maximum charge voltage limit (5% tolerance resistors were used). For this reason, it was assumed that the theoretical charge rate was matched by the experiment, successfully demonstrating the SMFCs functionality in-field, with potential for two charge cycles per day.

The final step was to use the electrical energy produced to treat water using an electrochemical reactor. For this, the SMFC stack was subsequently integrated with the electrochemical reactor and operated under the conditions optimised in the lab. The ability of the integrated system to treat the pond water was then investigated. The efficacy of treatment was confirmed by the change of colour of the water sample in the outlet (Figure S10). At BDD anodes, organic matter degradation is favoured independently of the applied current density, as already confirmed in lab tests (Figure 8). The process is controlled by mass transport, which is affected by the residence reactor time due to the flow rate (Figure 8), in agreement with previous studies (3). Efficient production of hydroxyl radicals is promoted at BDD surface, favouring the pollutants degradation close to anode surface and in the reaction cage. Unlike active anodes, BDD has higher oxygen evolution potential (+2.30 V versus SHE), and does not provide any catalytic

active sites for the adsorption of reactants and/or products from the aqueous solution. Instead, it favours the oxidation of water molecules, leading to the fast formation of free-hydroxyl radicals, as follows (3):

$$\mathrm{BDD}(^{\bullet}\mathrm{OH}) + \text{organic matter} \rightarrow \mathrm{BDD} + \mathrm{CO_2} + \mathrm{H_2}O$$

These species are weakly absorbed at the anode surface and are consequently available to react, favouring the electrochemical oxidation and mineralization of organics in the real water. Although characterised by a short life-time, hydroxyl radicals are available to attack pollutants (i.e. organic matter and microorganism), allowing the formation of intermediates that oxidize into CO_2 and H_2O (48, 51). It is important to highlight that, although the electrochemical oxidation using non-active anode is principally favoured by the free-hydroxyl radicals action, the presence of sulphate or chloride ions in the real water sample allows the electrogeneration of stable oxidizing species, such as persulfate and active chlorine, which also contribute to the abatement of organic substrates (3).

The electrochemical reactor caused an increase of over two folds in the dissolved oxygen (DO) of the outlet water. Before the treatment, the DO of the water was 3.2 ± 0.2 mg L^{-1} and after the electrochemical treatment was 7.7 mg L^{-1}, representative of the efficacy of the electrochemical treatment. Considering that a single battery charge could sustain the reactor operation for approximately 1.5 h, treating 1.4 L of water, the integrated system could treat an average of 2.8 L of water per day. Note, that in this proof-of concept study the main goal was to show that SMFCs can produce enough electricity under field conditions to operate a simple water purification system based on chemical oxidation. Further experiments are needed to test the disinfection performance of the system and its applicability to produce drinking water quality from various sources.

Conclusions

This work presents the first demonstration of the development and upscaling, from the lab to the field, of a stack of soil microbial fuel cells to generate renewable energy and power an electrochemical reactor for water treatment. The soil microbial fuel cells are characterised by a simple and low-cost design and operate in a shared electrolyte configuration. The power output is effectively increased by stacking multiple soil microbial fuel cell units, which proved to be a more effective scale-up strategy rather than increasing the electrode size. The soil microbial fuel cells showed a stable performance over several months of operation, provided that the soil water content is kept at approximately 50%. Despite differences in soil

composition, irrigation water and ambient temperature and humidity, the current generated by the stack of 16 soil microbial fuel cells in the field was within 12% of the current produced in the lab. The current at peak power output generated by the stack of 64 fuel cells in the field was of estimated to be 85 mA. When connected to the power management system, the soil microbial fuel cells were able to charge a 600 mAh battery in roughly 8.5 h. The battery could sustain the reactor operation for 1.5 h, treating 1.4 L of water. Therefore, the integrated system was capable of treating up to 2.8 L of water per day with an electrochemical advanced oxidation process. Since the soil microbial fuel cells were operated in air-cathode mode and irrigated by a gravity fed set-up, there was no need for aeration or pumping. The developed integrated system can, therefore, provide a sustainable decentralised solution for power generation and the self-powered treatment of water in remote areas.

Acknowledgments

The authors acknowledge: the University of Bath to fund Jakub Dziegielowski's PhD scholarship; Research England to fund the project SmARTER (Sustainable Approaches for Resilience Building in North East Brazil), through the Global Challenges Research Fund (Research England QR GCRF); CNPq/Nexus I Proc. nº 441489/2017-6 "Tecnologias sociais e ações integradas de sustentabilidade para a garantia da segurança hídrica, energética e alimentar em nível comunitário no semiárido cearense"CNPq/Nexus I Proc. 441489/2017-6, to fund the project project 'Tecnologia sociais e acoes integrada de sustenabilidades para garantia da seguranca hidrica energetica e alimentar em nivel comunitario no semiarido cearence'; PRINT/CAPES Proc. nº 88887.312019/2018-00 "Integrated socio-environmental technologies and methods for territorial sustainability: alternatives for local communities in the context of climate change".

The authors also thank teachers and pupils of the primary school EEF Professora Mizinha of Icapuí, State of Ceará, Brazil, without whom the field test could have not been performed.

References

1. A P-Ü, Bos R, Gore F, Bartram J. Safer water, better health: costs, benefits and sustainability of interventions to protect and promote health. Geneva: World Health Organization; 2008. p. 1-60.
2. Gutiérrez APA, Engle NL, Nys ED, Molejón C, Martins ES. Drought preparedness in Brazil. Weather and Climate Extremes. 2014;3:95-106.
3. Martínez-Huitle CA, Panizza M. Electrochemical oxidation of organic pollutants for wastewater treatment. Current Opinion in Electrochemistry. 2018;11:62-71.
4. T. S, McBeath, P. D, Wilkinson, D. NJ, Graham. Application of boron-doped diamond electrodes for the anodic oxidation of pesticide micropollutants in a water treatment process: a critical review Environmental Science: Water Research & Technology. 2019;5(12):2090-107.
5. Ganiyu SO, Zhou M, Martínez-Huitle CA. Heterogeneous electro-Fenton and photoelectro-Fenton processes: A critical review of fundamental principles and application for water/wastewater treatment. Applied Catalysis B: Environmental. 2018;Volume 235:103-29.
6. Martínez-Huitle CA, Manuel A, Ignasi R, Scialdone SO. Single and Coupled Electrochemical Processes and Reactors for the Abatement of Organic Water Pollutants: A Critical Review. Chemical Reviews. 2015;115(24):13362-407.
7. Ganiyu SO, Martínez-Huitle CA, Rodrigo MA. Renewable energies driven electrochemical wastewater/soil decontamination technologies: A critical review of fundamental concepts and applications. Applied Catalysis B: Environmental. 2020;270.
8. Monasterio S, Mascia M, Lorenzo MD. Electrochemical removal of microalgae with an integrated electrolysis-microbial fuel cell closed-loop system. Separation and Purification Technology. 2017;183(7):373-81.
9. Santoro C, Arbizzani C, Erable B, Ieropoulos I. Microbial fuel cells: From fundamentals to applications. A review. Journal of Power Sources. 2017;356:225-44.
10. Hiegemann H, Littfinski T, Krimmler S, Lübken M, Klein D, Schmelz KG, et al. Performance and inorganic fouling of a submergible 255 L prototype microbial fuel cell module during continuous long-term operation with real municipal wastewater under practical conditions. Bioresource Technology. 2019;294.
11. Samrat N, Rao K, Ruggeri B, Tommasi T. Denitrification of water in a microbial fuel cell (MFC) using seawater bacteria. Journal of Cleaner Production. 2018;178:449-56.
12. Ieropoulos I, Pasternak G, Greenman J. Urine disinfection and *in situ* pathogen killing using a Microbial Fuel Cell cascade system. PLoS ONE; 2017.
13. Gosselin F, Madeira LM, Juhna T, Block JC. Drinking water and biofilm disinfection by Fenton-like reaction. Water Research. 2013;47(15):5631-8.
14. Gajda I, Greenman J, Ieropoulos I. Recent advancements in real-world microbial fuel cell applications. Current Opinion in Electrochemistry. 2018;11:78-83.
15. Song YE, Boghani HC, Kim HS, Kim BG, Lee T, Jeon BH, et al. Maximum Power Point Tracking to Increase the Power Production and Treatment Efficiency of a Continuously Operated Flat-Plate Microbial Fuel Cell. Energy Technology. 2016;4(11):1427-34.
16. Castresana PA, Martinez SM, Freeman E, Eslava S, Lorenzo MD. Electricity generation from moss with light-driven microbial fuel cells. Electrochimica Acta. 2019;298:934-42.
17. Flimban SGA, Ismail IMI, Kim T, Oh S. Overview of Recent Advancements in the MicrobialFuel Cell from Fundamentals to Applications: Design, Major Elements, and Scalability. Energies. 2019;12.

18. Nitisoravut R, Regmi R. Plant microbial fuel cells: A promising biosystems engineering. Renewable and Sustainable Energy Reviews. 2017;76:81-9.
19. Chen Z, Huang Y, Liang J, Zhao F, Zhu Y. A novel sediment microbial fuel cell with a biocathode in the rice rhizosphere. Bioresource Technology. 2012;108:55-9.
20. Erable B, Lacroix R, Etcheverry L, Féron D, Delia ML, Bergel A. Marine floating microbial fuel cell involving aerobic biofilm on stainless steel cathodes. Bioresource Technology. 2013;142:510-6.
21. Dumas C, Basseguy R, Bergel A. DSA to grow electrochemically active biofilms of G*eobacter sulfurreducens*. Electrochimica Acta. 2008;53(7):3200-9.
22. Wetser K, iu JL, Buisman C, Strik D. Plant microbial fuel cell applied in wetlands: Spatial, temporal and potential electricity generation of S*partina anglica* salt marshes and P*hragmites australis* peat soils. Biomass and Bioenergy. 2015;83:543-50.
23. Takanezawa K, Nishio K, Kato S, Hashimoto K, Watanabe K. Factors affecting electric output from rice-paddy microbial fuel cells. Bioscience, Biotechnology and Biochemistry. 2010;74(6):1271-3.
24. Moqsud MA, Omine K. Assessment of factors influencing bioelectricity generation in paddy plant microbial fuel cells. Global Advanced Research Journal of Agricultural Science. 2015.
25. Kabutey FT, Zhao Q, Wei L, Ding J, Antwi P, Quashie FK, et al. An overview of plant microbial fuel cells (PMFCs): Configurations and applications. Renewable and Sustainable Energy Reviews. 2019;110:402-14.
26. Liu S, Song H, Li X, Yang F. Power Generation Enhancement by Utilizing Plant Photosynthate in Microbial Fuel Cell Coupled Constructed Wetland System. International Journal of Photoenergy. 2013:10.
27. Kaku N, Yonezawa N, Kodama Y, Watanabe K. Plant/microbe cooperation for electricity generation in a rice paddy field. Applied Microbiology and Biotechnology. 2008;**79**:43 – 9.
28. Wetser K, Dieleman K, Buisman C, Strik D. Electricity from wetlands: Tubular plant microbial fuels with silicone gas-diffusion biocathodes. Applied Energy. 2017;185:642-9.
29. Tapia NF, Rojas C, Bonilla CA, Vargas IT. Evaluation of S*edum* as driver for plant microbial fuel cells in a semi-arid green roof ecosystem. Ecological Engineering. 2017;108:203-10.
30. Amari S, Vahdati M, Ebadi T. Investigation into effects of cathode aeration on output current characteristics in a tubular microbial fuel cell. International Journal of Science and Technology. 2015;12:4037–42.
31. Horneck DA, Sullivan DM, Owen JS, Hart JM. Soil Test Interpretation Guide. Oregon State University2011.
32. Jim R, Mike M. Moisture content by the oven-dry method for industrial testing. Oregon State University, Corvallis, OR1999.
33. Konare H, Yost R, Doumbia M, Mccarty GW, Jarju A, Kablan R. Loss of ignition: Measuring soil organic carbon in soils of the Sahel, West Africa. African journal of agricultural research. 2010;5(22):3088-95.
34. Monasterio S, Lorenzo MD. Electricity generation from untreated fresh digestate with a cost-effective array of floating microbial fuel cells. Chemical Engineering Science. 2019;198:108-16.
35. Al-Qaradawi S, Salman SR. Photocatalytic degradation of methyl orange as a model compound. Journal of Photochemistry and Photobiology. 2002;148:161–8.
36. Instruments T. BQ25504 Ultra Low-Power Boost Converter With Battery Management For Energy Harvester Applications. 2019.

37. Zhuang L, Zhou S. Substrate cross-conduction effect on the performance of serially connected microbial fuel cell stack. Electrochemistry Communications. 2009;11(5):936-40.
38. Kim D, An J, Kim B, Kim BH. Scaling-Up Microbial Fuel Cells: Configuration and Potential Drop Phenomenon at Series Connection of Unit Cells in Shared Anolyte. CHEMSUSCHEM. 2012;5:1086-91.
39. Chouler J, Padgett GA, Cameron PJ, Preuss K, Titirici M-M, Ieropoulos I, et al. Towards effective small scale microbial fuel cells for energy generation from urine. Electrochemica Acta. 2016;192:89-98.
40. Lim KG, Tayhas G, Palmore R. Microfluidic biofuel cells: The influence of electrode diffusion layer on performance. Biosensors and Bioelectronics. 2007;22(6):941-7.
41. Molognoni D, Colprim J. Reducing start-up time and minimizing energy losses of Microbial Fuel Cells using Maximum Power Point Tracking strategy. Journal of Power Sources. 2014;268:403-11.
42. Hamdi A, Ramtin NR, Mohammad S. Fuel Cells. Design, Operation and Grid Integration2017. p. 221-300.
43. Dewan A, Beyenal H, Lewandowski Z. Scaling up Microbial Fuel Cells. Environmental Science Technology. 2008;42:7643-8.
44. Pasternak G, Greenman J, Ieropoulos I. Dynamic evolution of anodic biofilm when maturing under different external resistive loads in microbial fuel cells. Electrochemical perspective. Journal of Power Sources. 2018;400:392-401.
45. Lu L, Xing D, Ren ZJ. Microbial community structure accompanied with electricity production in a constructed wetland plant microbial fuel cell. Bioresource Technology. 2015;195:115-21.
46. Martinucci E, Pizza F, Perrino D, Colombo A, Trasatti SPM, Barnabei AL, et al. Energy balance and microbial fuel cells experimentation at wastewater treatment plant Milano-Nosedo. International Journal of Hydrogen Energy. 2015;40(42):14683-9.
47. Martinez-Huitle CA, Brillas E. Decontamination of wastewaters containing synthetic organic dyes by electrochemical methods: A general review. Applied Catalysis B: Environmental. 2009;87(3-4):105-45.
48. Martínez-Huitle CA, Rodrigo MA, Scialdone O. Electrochemical Water and Wastewater Treatment. 1 ed2018. 556 p.
49. Rodrigo MA, Oturan N, Oturan MA. Electrochemically Assisted Remediation of Pesticides in Soils and Water: A Review. Chemical Reviews. 2014;114(17):8720-45.
50. Benjamin K, Luis RF, Falk H, Cristian P. A framework for modeling electroactive microbial biofilms performing direct electron transfer. Bioelectrochemistry. 2015;106:194-206.
51. Martínez-Huitle CA, Brillas E. Electrochemical Alternatives for Drinking Water Disinfection. Angewandte Chemie International Edition. 2008;47(11): 1998-2005.

Development of a functional stack of soil microbial fuel cells to power a water treatment reactor: from the lab to field trials in North East Brazil

Jakub Dziegielowski, Benjamin Metcalfe, Paola Villegas-Guzmán, Carlos A. Martínez-Huitle, Adryane Gorayeb, Jannis Wenk, Mirella Di Lorenzo

Supplementary data

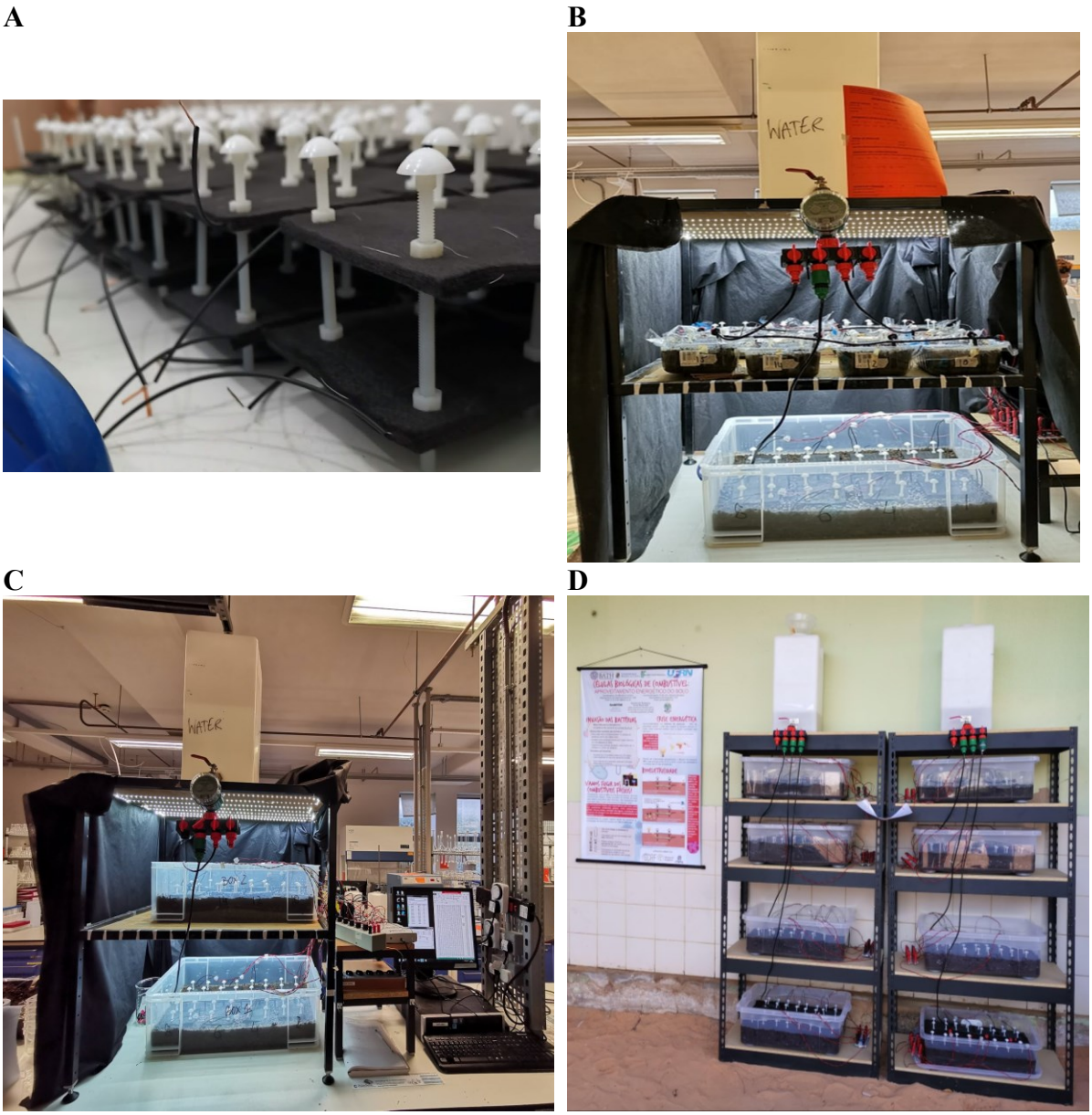

Figure S1. Experimental designs implemented throughout the study. A) SMFC reactor design used in majority of the experiments; B) Laboratory set-up of the individual vs. shared anolyte SMFCs; C) Laboratory set-up of the 16 SMFC stack connected in parallel; D) Field-based set-up comprising of 64 SMFCs connected in parallel.

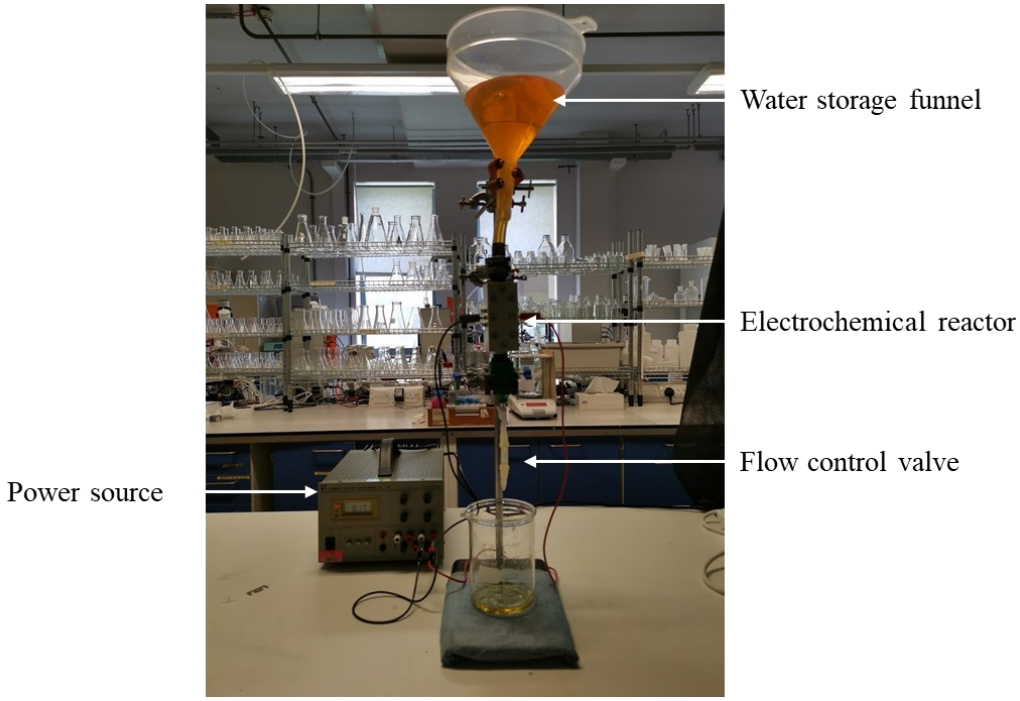

Figure S2. Gravity driven set-up for electrochemical water treatment.

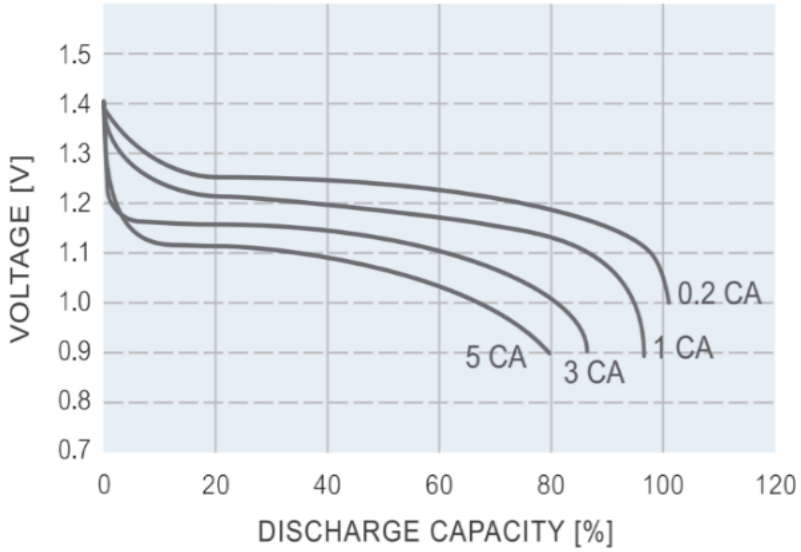

Figure S3. Discharge curves of single cell NiMH battery adapted in the study. CA refers to discharge current (1 CA = 100 mA).

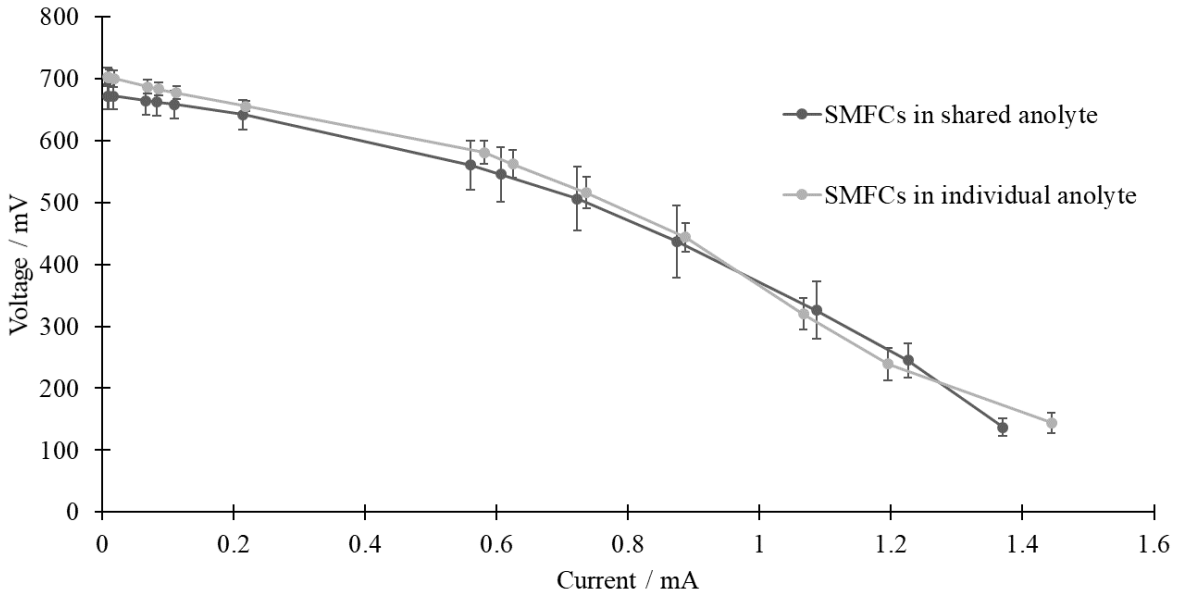

Figure S4. Polarization curves comparing the performance of single SMFC in shared vs. individual anolyte system. The results were obtained from polarization tests performed after 25 days of operation. Error bars refer to four replicates.

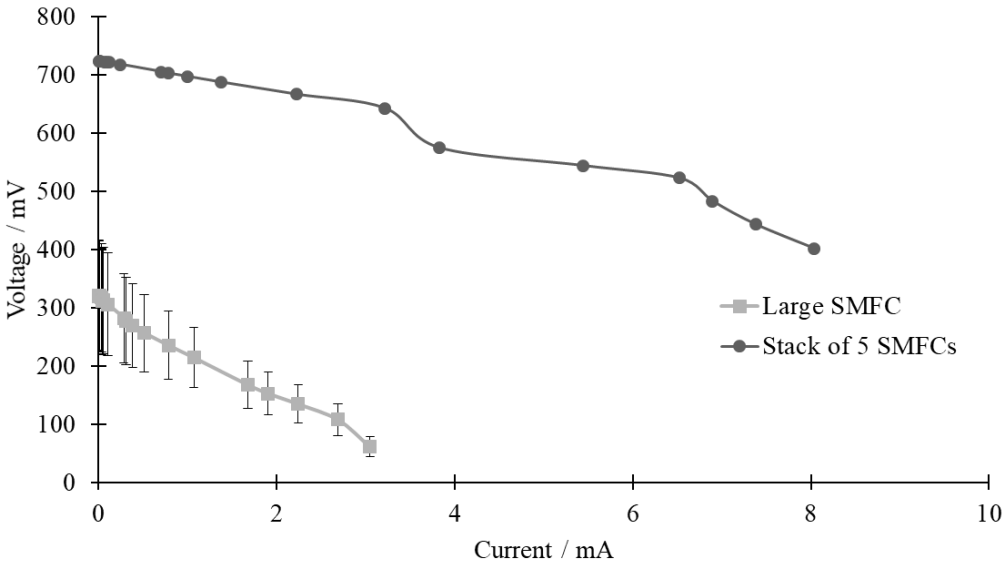

Figure S5. Polarization curves comparing the performance of a large SMFC vs. a stack of 5 smaller units, connected in parallel.

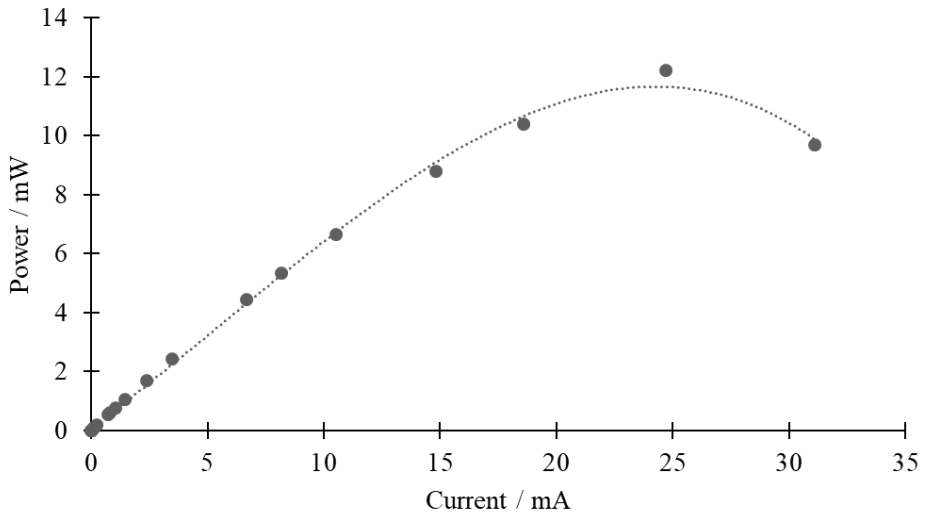

Figure S6. Power curve obtained by stacking 16 SMFCs in shared anolyte conditions. The values were obtained through polarisation tests, as described in the Methods section. The polarisation was performed after 70 days of operation.

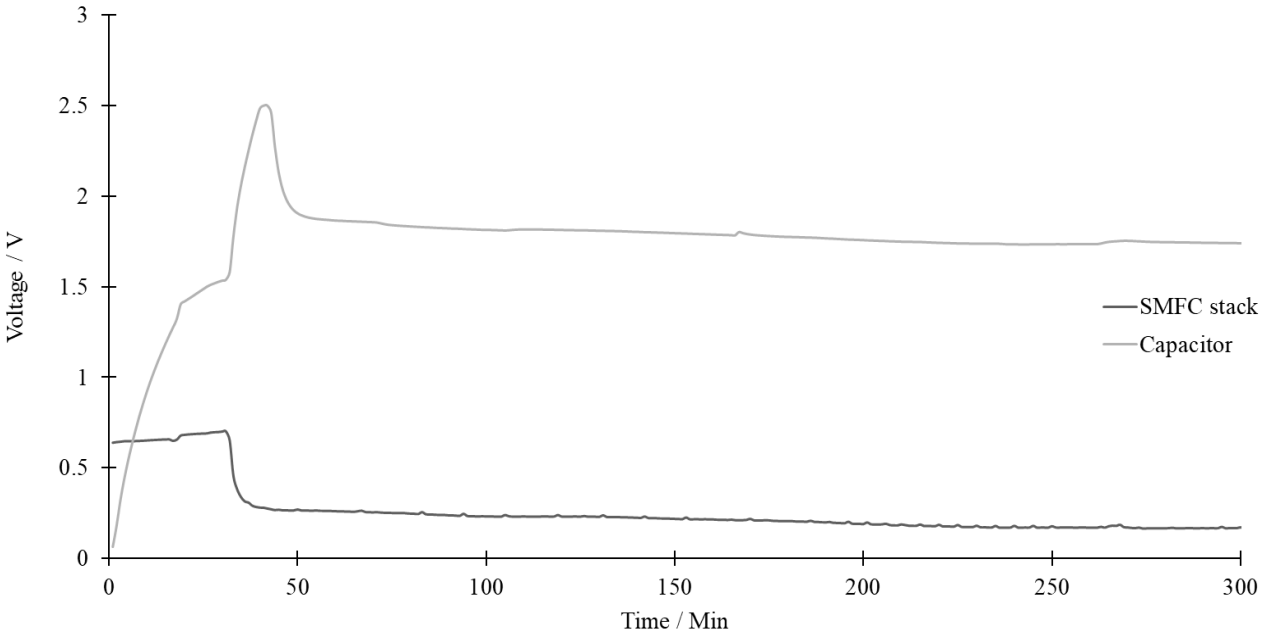

Figure S7. Charge and discharge test during which the fuel cells were connected to the energy harvester. The electricity was stored in a 470 µF capacitor and dissipated to a LED. The obtained results show that at the initial stages of charging the capacitor, the SMFCs voltage was very high, displaying OCV behaviour, which indicates the absence of an external load.

Once the capacitor reached a voltage of 1.5 V, the voltage of the SMFC stack dropped by over 50%. This rapid drop in voltage suggests that at this point the energy harnessing system applied a resistance to maximise the power generation from the SMFCs. This is backed up by the behaviour of the capacitor, as at this point, the charge rate increased significantly. Once the capacitor reached its full charge at around 2.5 V, the LED was connected to the system. As soon as the LED lit up, the capacitor's voltage dropped to 1.8 V, and subsequently a steady state value of approximately 1.7 V was reached. The LED remained lit throughout the whole test, thus implying that the SMFCs stack was powerful enough to sustain continuous powering, and that the energy harnesser was functional with the system.

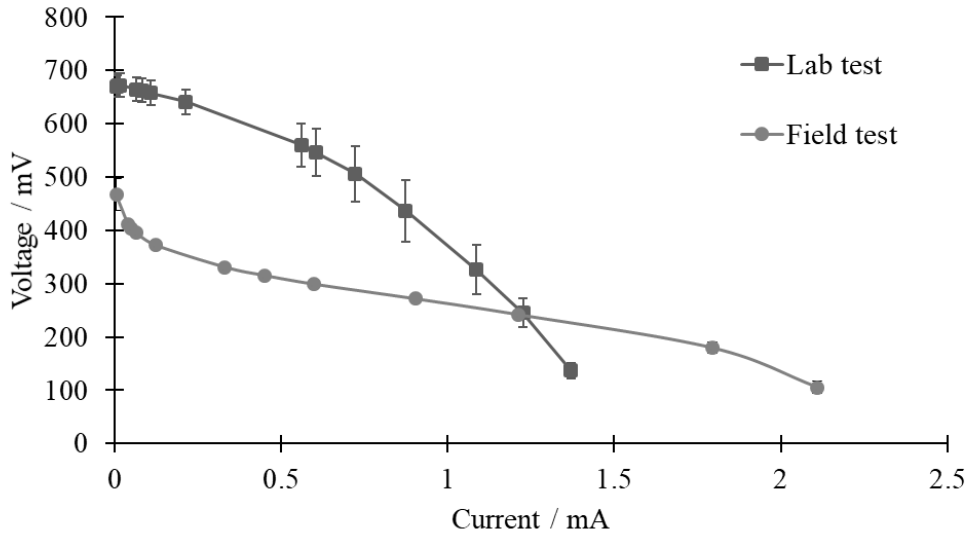

Figure S8. Polarization curves comparing the performance of single SMFC in the lab vs. field-based system.

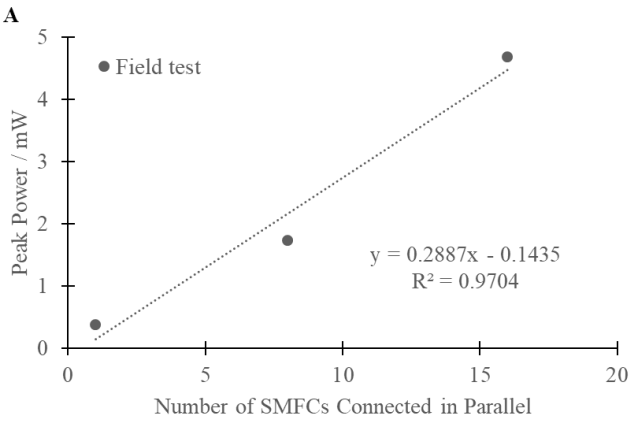
A
Field test
Peak Power / mW
y = 0.2887x - 0.1435
R² = 0.9704
Number of SMFCs Connected in Parallel

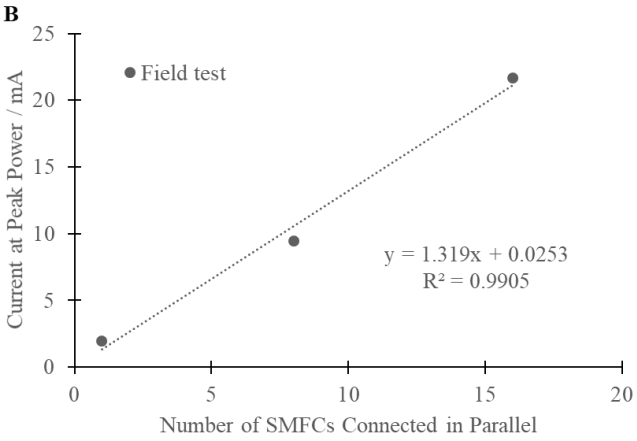
B
Field test
Current at Peak Power / mA
y = 1.319x + 0.0253
R² = 0.9905
Number of SMFCs Connected in Parallel

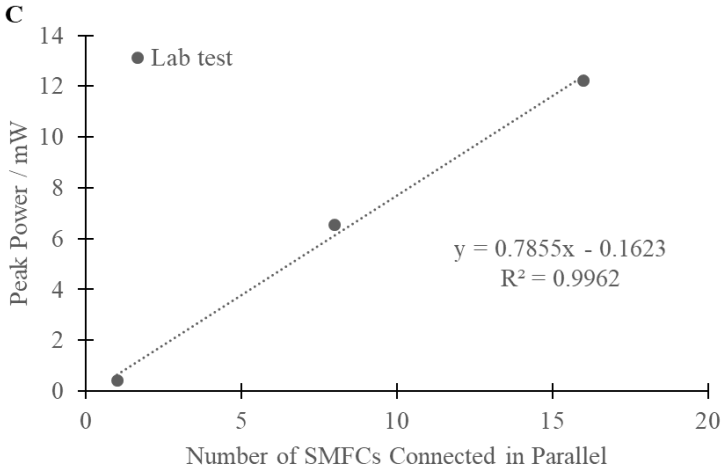
C
Lab test
Peak Power / mW
y = 0.7855x - 0.1623
R² = 0.9962
Number of SMFCs Connected in Parallel

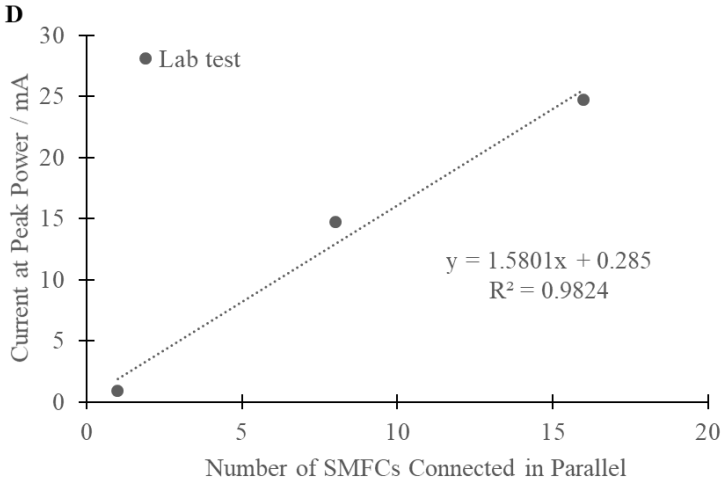
D
Lab test
Current at Peak Power / mA
y = 1.5801x + 0.285
R² = 0.9824
Number of SMFCs Connected in Parallel

Figure S9. Linear relation between peak power and current vs. number of SMFCs stacked in parallel obtained during (A-B) field tests and (C-D) lab tests, respectively.

A

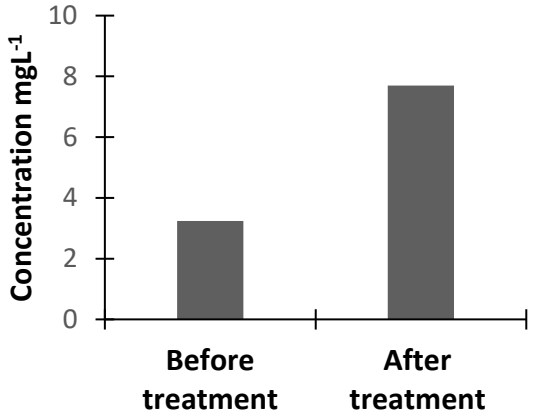

B

Figure S10. A) Dissolved oxygen of the pond water before and after treatment with the integrated system. B) Colour change of pond water before and after treatment